ISSN 1024-8560, Atmospheric and Oceanic Optics, 2022, Vol. 35, No. 6, pp. 782–792. © Pleiades Publishing, Ltd., 2022.
Russian Text © The Author(s), 2022, published in Optika Atmosfery i Okeana.

OPTICAL MODELS AND DATABASES

Scale Heights of Water Vapor and Sulfur Compounds in the Lower Troposphere

A. V. Eliseev[a, b, c, d, *], A. V. Timazhev[b, **], and P. L. Jimenez[c, *]**

[a] *Moscow State University, Moscow, 119991 Russia*
[b] *Obukhov Institute of Atmospheric Physics, Russian Academy of Sciences, Moscow, 119017 Russia*
[c] *Kazan Federal University, Kazan, 420097 Russia*
[d] *Institute of Applied Physics, Russian Academy of Sciences, Nizhny Novgorod, 603950 Russia*
**e-mail: eliseev.alexey.v@gmail.com*
***e-mail: timazhev@ifaran.ru*
****e-mail: leonardojimenez1990@gmail.com*

Received February 25, 2022; revised April 12, 2022; accepted May 16, 2022

Abstract—A global analysis of geographical features of vertical profiles of specific air humidity and concentrations of sulfur dioxide and sulfate aerosols is carried out based on the CAMS reanalysis data, as well as the height of the planetary boundary layer (PBL) based on the ERA5 reanalysis data for 2003–2020. The scale height H_Y, i.e., the height at which the concentration of the substance Y decreases by a factor of e, is used as a characteristic of the aforesaid profiles. The maximal heights of the upper PBL boundary are observed in regions of the prevailing cyclonic gyre—in storm tracks and in regions of monsoonal circulation in summer. For the vertical scale of the specific humidity profile, minima are identified in the regions of the subtropical gyre with prevailing large-scale subsidence of air masses. The scale height of SO_2 is characterized by spatial minima associated with oxidation of this substance. For H_{SO_4}, a spatial minimum over the ocean near southeast Asia is found. A statistically significant negative correlation between the PBL thickness and the vertical scale of the specific humidity profile in humid regions of the tropics is revealed, as well as a positive correlation between scale heights of sulfur dioxide and sulfates, most significantly manifested in regions with acute pollution of the lower troposphere by these substances.

Keywords: sulfur dioxide, sulfates, specific humidity, vertical scale, planetary boundary layer, correlation relationships

DOI: 10.1134/S1024856022060100

INTRODUCTION

One of the features of the Earth's lower troposphere is the universal structure of vertical profiles of atmospheric impurities, the sources of which are situated on the Earth's surface [1–3]. The dependence on altitude above the surface z, both for the concentration and for the mixing ratio, has the form

$$q_Y(z) = q_Y(0)\exp(-z/H_Y), \quad (1)$$

where the subscript Y points to a substance and H_Y is the height scale of this substance, i.e., the height at which concentration of the substance Y decreases by a factor of e. Relationship (1) allows one, in particular, to relate the total content of this impurity in a column with a unit area to its ground level concentration [4]:

$$B_Y = q_Y(0)H_Y. \quad (2)$$

For this purpose, it is necessary that $H_Y < H$, where H is the atmospheric density scale height. In turn, Eqs. (1) and (2) can be used in simplified models of the atmosphere, in particular, in Earth system models of intermediate complexity [5–11]. Models of this class are often formulated under the assumption that time scales for processes determining the structure of the vertical profile $q_Y(z)$ are notably less than time scales of processes explicitly resolved by such model [5, 7].

Relationship (1) can be justified under simultaneous fulfillment of two conditions: (i) the sources (emission and/or chemical formation) of an impurity are on the Earth's surface and (ii) the vertical transfer of the impurity is a result of two processes—diffusion and gravity sedimentation [2]. However, this relationship can be also valid for substances for which humid washout dominates in the release from the atmosphere, e.g., for sulfate aerosols [1, 2] or water vapor [3].

The scale height H_Y can significantly depend not only on the choice of the substance Y but also on the state of the atmospheric boundary layer, i.e., on the

geographical point and time. Such variations were observed, in particular, in [1]. At the simplest level, their causes can be understood from the theory of dry deposition of atmospheric impurities [2]. According to this theory,

$$H_Y = H/\left(1 + u_{T,Y}H/K_{z,Y}\right), \quad (3)$$

where $u_{T,Y}$ is the terminal velocity (depending on the density of impurity particles, their size, and shape) and $K_{z,Y}$ is the coefficient of vertical diffusion for the substance Y, constant over altitude. In view of the relation between the coefficient of diffusion $K_{z,Y}$ and stratification features of the planetary boundary layer (PBL), it is possible that $0 \le H_Y \le H$.

It should also be kept in mind that the height of the upper boundary of the PBL relative to the Earth H_{BL} depends on the coefficient of diffusion for the momentum in dry air $K_{z,\,air}$ [12]. In particular, in the Eckman approximation for the PBL, it is valid that

$$H_{BL,E} = (2K_{z,air}/f)^{1/2}, \quad (4)$$

where f is the Coriolis parameter. With allowance for the relation between coefficients of molecular diffusion for different substances and their molecular masses [13], one can assume that all $K_{z,Y}$ (including $K_{z,\,air}$) at the given PBL state differ from each other only by constant coefficients (depending only on the substance Y). Thus, proceeding from Eqs. (3) and (4), one can expect a positive correlation between H_Y and H_{PBL}.

This work is aimed at analyzing scale heights of sulfate aerosols ($Y = SO_4$) and their main chemical precursor, sulfur dioxide ($Y = SO_2$). In addition, the value of H_Y is analyzed for water vapor (Y = vap). The last is related both to the use of relationship (1) for describing the vertical distribution of water vapor in the troposphere [3] and with the importance of this variable for chemical transformations of sulfur compounds in the atmosphere [4, 14]. Finally, this work analyzes the height of the upper PBL boundary relative to the Earth's surface H_{PBL}.

All analyzed impurities directly affect optical properties of the atmosphere. Water vapor is the strongest greenhouse gas [15]; it also has an effect on optical properties of the atmosphere in the solar range [15]. Moreover, its content in the atmosphere affects the formation of clouds which modify the transfer of solar and thermal radiation [15, 16]. Sulfate aerosols also have a significant effect on the solar radiation transfer in the Earth's atmosphere due to direct scattering of solar radiation and modification of cloudiness characteristics [15, 17, 18]. Sulfur dioxide is the most important chemical precursor of sulfate aerosols [2]. It has an effect on vegetation photosynthesis and, indirectly, on the atmospheric content of carbon dioxide, which is one more important greenhouse gas [14, 19–21].

1. MATERIALS AND METHODS

The analysis was performed based on the monthly average data of the Copernicus Atmospheric Monitoring Service (CAMS) [22] and ERA5 reanalyses [23] for 2003–2020. From the first data array, specific humidity (variable q in the CAMS nomenclature) and mixing ratios for sulfur dioxide (SO_2) and sulfate aerosol (aermr11) at isobaric levels in the layer from 950 to 600 hPa were used for the analysis. In view of the fact that all abovementioned gases are trace atmospheric gases, the mixing ratio for them was assumed to be equivalent to the concentration. Besides, the height of the upper PBL boundary was analyzed (variable blh in the ERA5 nomenclature). Note that the height of the upper PBL boundary in the ERA5 reanalysis is defined as the minimal altitude above the Earth's surface at which the Richardson number reaches 0.25 [24].

Specific humidity and concentrations of sulfur dioxide and sulfate aerosol were approximated by relationship (1) in the form of linear regression $\ln(q_Y(z)/q_Y(0))$, the coefficients of which were estimated using the regCoef_n function of the NCL (NCAR Command Language) package. The altitude z was reckoned from sea level and was approximated by a quantity proportional to $\ln(p/p_0)$, where p is the pressure at the given isobaric level and $p_0 = 950$ hPa. The grid nodes with orography above the isobaric level p_0, as well as with $H_Y > 3$ km, were excluded from the consideration. The last is related to the fact that either the concentration of the substance Y is low relative to other regions (and, therefore, the vertical profile of this concentration is hard to measure) or there appear inversions in the PBL (which makes relationship (1) inapplicable) at such nodes.

Calculation of global and annual average values of all H_Y (denoted in what follows as $H_Y^{(g)}$) in this work is carried out only at grid nodes not excluded from consideration for reasons given above.

2. RESULTS

2.1. Long-Term Annual Average Values of the Planetary Boundary Layer Thickness and Scale Heights for Atmospheric Impurities

The PBL height relative to the Earth's surface is characterized by lower values over land and ocean in high and subpolar latitudes (up to 0.7 km) as compared to the ocean in lower latitudes (from 0.6 to 1.8 km) (Fig. 1). In regions of intense synoptic activity (in particular, in regions of storm tracks) characterized by the cyclonic gyre with ascending air masses in the lower troposphere, the PBL heights are maximal. In the last case, an increase in H_{BL} is also visible in winter of the corresponding hemisphere, when synoptic processes are more active than in summer.

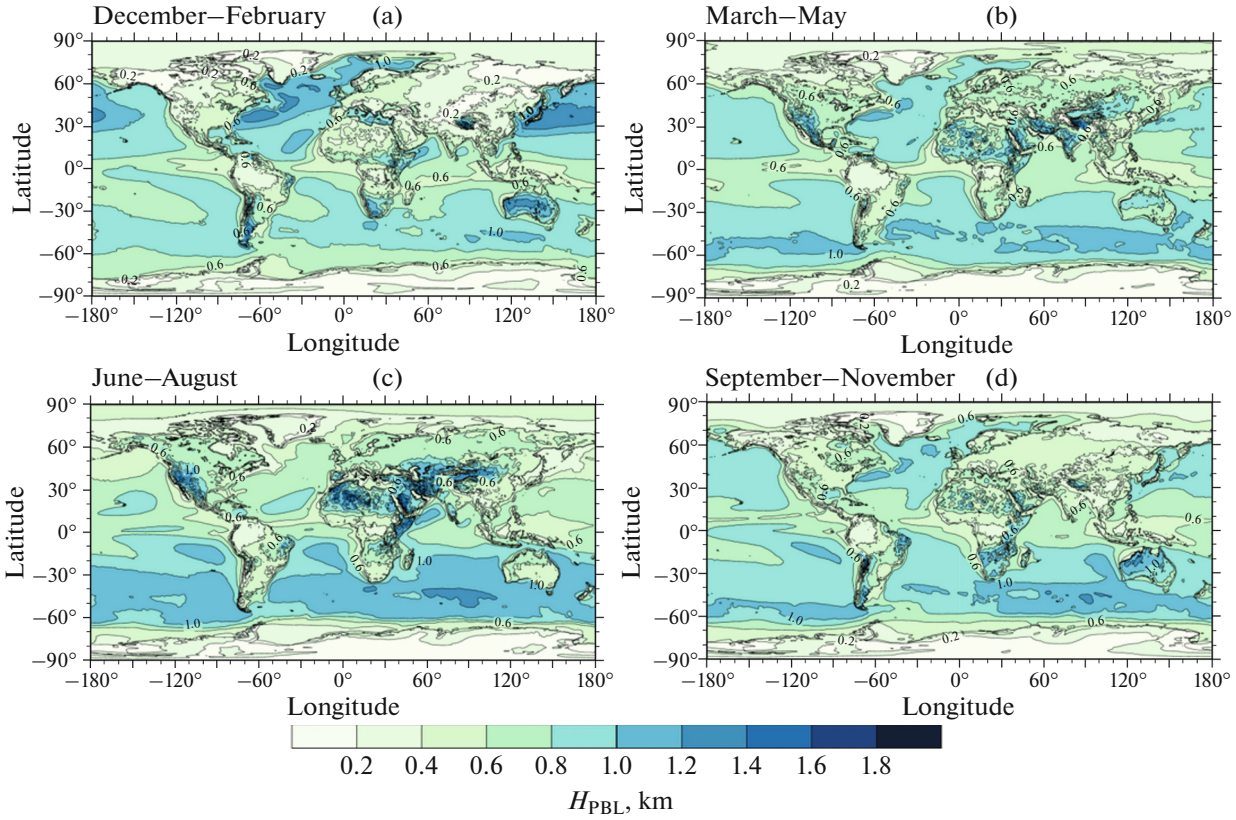

Fig. 1. Seasonal average height of the PBL boundary relative to the Earth's surface for 2003–2020 (a) in Northern Hemisphere winter, (b) in spring, (c) in summer, and (d) in autumn.

In summer, the H_{PBL} maximum is also found in the south and southeast of Eurasia. In some regions, the maximum exceeds 1.8 km (Fig. 1c). It is related to the development of the monsoonal cyclonic circulation in this season. The aforesaid maximum manifests itself to a lesser extent in spring (Fig. 1b).

It should be noted that, according to Eq. (4), such change in the PBL can be interpreted as an increase in $K_{z,\ air}$ during strong cyclonic activity [25], which is shown in the development of convective processes in the PBL thickness.

The vertical scale for specific humidity H_{vap} over oceans lies as a rule in the range 1.4–2.2 km (Fig. 2). The minima are observed in regions of subtropical gyres with predominance of anticyclonic conditions, i.e., with predominating large-scale subsidence of air masses. In winter, H_{vap} is in general lower than in summer.

Over land, values of H_{vap} exceed those over oceans: from 2.2 km and higher. In contrast to oceanic regions, the vertical scale for specific humidity in winter is higher than in summer.

The interannual root-mean-square deviation (IRMSD) of seasonal average values of H_{vap} in most regions is ~0.1 km, with the exception of regions of the intratropical convergence zone (ITCZ), where it can reach 0.3 km.

Under global and annual averaging, $H_{vap}^{(g)} = 2.5 \pm 0.1$ km.

The annual cycle of the scale height of sulfur dioxide H_{SO_2} over land is relatively feebly marked. However, a significant difference between regions with higher and lower contamination of the atmosphere by sulfur dioxide is observed. In the first case (south and southeast of Asia, Europe, and the east of North America), this scale height varies within the range from 0.6 to 2.2 km (Fig. 3).

Over the ocean, minimums of H_{SO_2} are observed in tropics—not more than 1.5 km, just as over regions with high contamination of the troposphere by sulfates (Figs. 5c, 5e; 6c, 6e; and 7c, 7e from [4]). The last seems to point to the influence of chemical oxidation of sulfur dioxide with formation of sulfate aerosols on the vertical scale.

The IRMSD of H_{SO_2} over the ocean is notably larger than the corresponding value for specific humidity. Over most oceanic regions, it varies from 0.3 to 0.5 km; in the ITCZ region, it can even exceed 1.0 km. Such large values are also observed over the

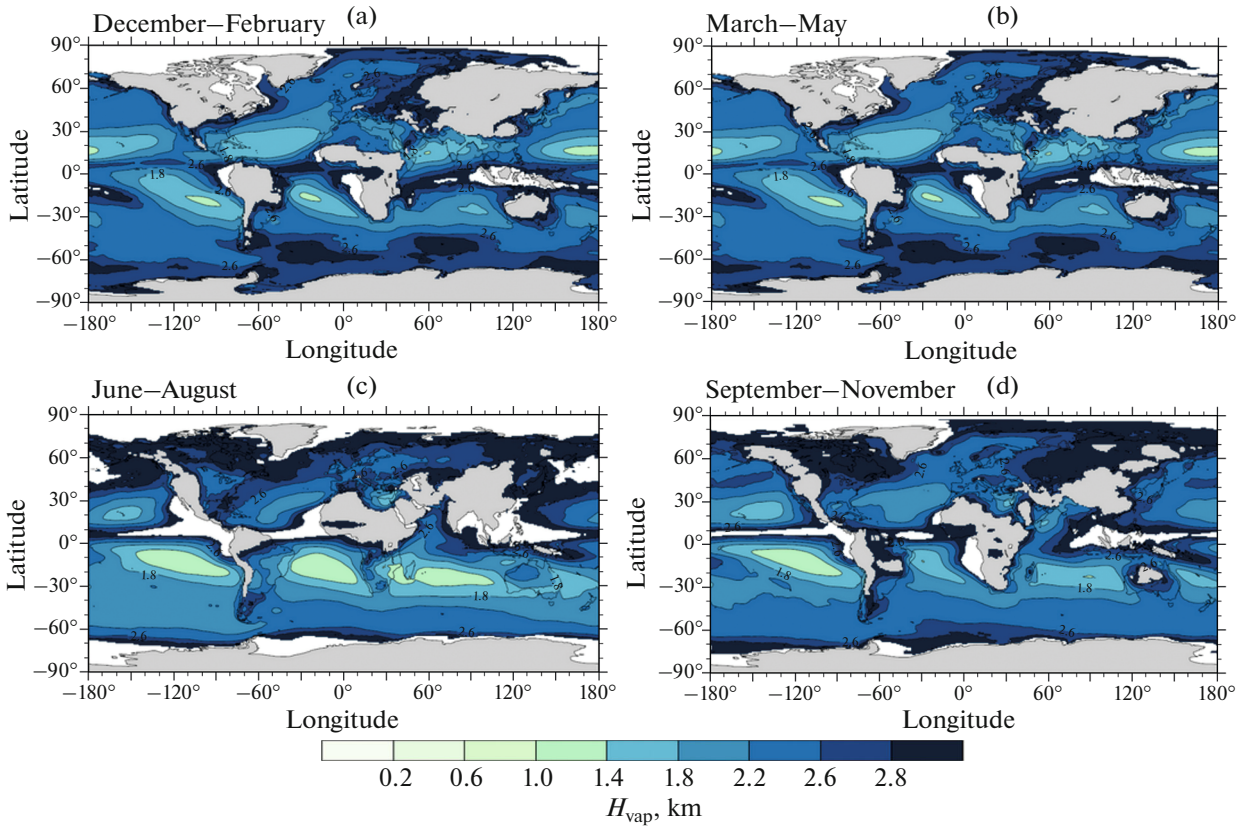

Fig. 2. Same as in Fig. 1 for the vertical scale of specific humidity (a) in Nortern Hemisphere winter, (b) in spring, (c) in summer, and (d) in autumn.

Arctic Ocean in summer. Over land, the IRMSD of H_{SO_2}, as a rule, does not exceed 0.3 km. On global and annual averaging, $H^{(g)}_{SO_2} = 2.6 \pm 0.2$ km.

The scale height of sulfates H_{SO_4} is determined worse than for other variables analyzed in this work: both over oceans and over continents, a large number of grid nodes are forcibly excluded from consideration (Fig. 4). For example, the scale height of sulfates is insufficiently reliably determined over most oceanic regions (with the exception of the ITCZ), as well as over most of land. This, in particular, impedes the analysis of the annual variation in H_{SO_4}.

In most regions where it was possible to calculate this scale height, it exceeded 1.8 km. However, the oceanic region near south and southeast Asia, where H_{SO_4} is close to 1.5 km, is an exception. This region is characterized by high aerosol contamination. The spatial H_{SO_4} minimum revealed here is hardly related to the rapid washout of sulfate aerosol by monsoon precipitations: this precipitation is most significant in summer, while the abovementioned spatial minimum is most pronounced in winter.

Similarly for specific humidity, the IRMSD of H_{SO_4} is equal to 0.1–0.3 km. Values over land are usually in the lower part of the abovementioned interval; over the ocean, in the upper part. In the case of global and annual averaging, $H^{(g)}_{SO_4} = 2.1 \pm 0.2$ km.

2.2. Relation between the Thickness of the Surface Boundary Layer and Vertical Scale for Specific Humidity

Using the fldcor and timcor functions of the CDO library (Climate Data Operators, http://doi.org/10.5281/zenodo.5614769), correlation relationships between scale heights and their connection with the PBL thickness were analyzed.

The spatial correlations between the variables are weak (Table 1). An exception is the negative correlation between H_{PBL} and H_{vap}, which corresponds to the time correlation in sign. In particular, the coefficients of the interannual correlation between H_{PBL} and H_{vap} calculated by seasonal average data turn out to be statistically significant in some tropical regions (Figs. 5 and 6). Note that at a series length of 18 years, without regard to autocorrelation and under the assumption of the normal distribution of interannual variations for all H_Y, the threshold values of the correlation coefficients for statistical significance levels of 90, 95, and

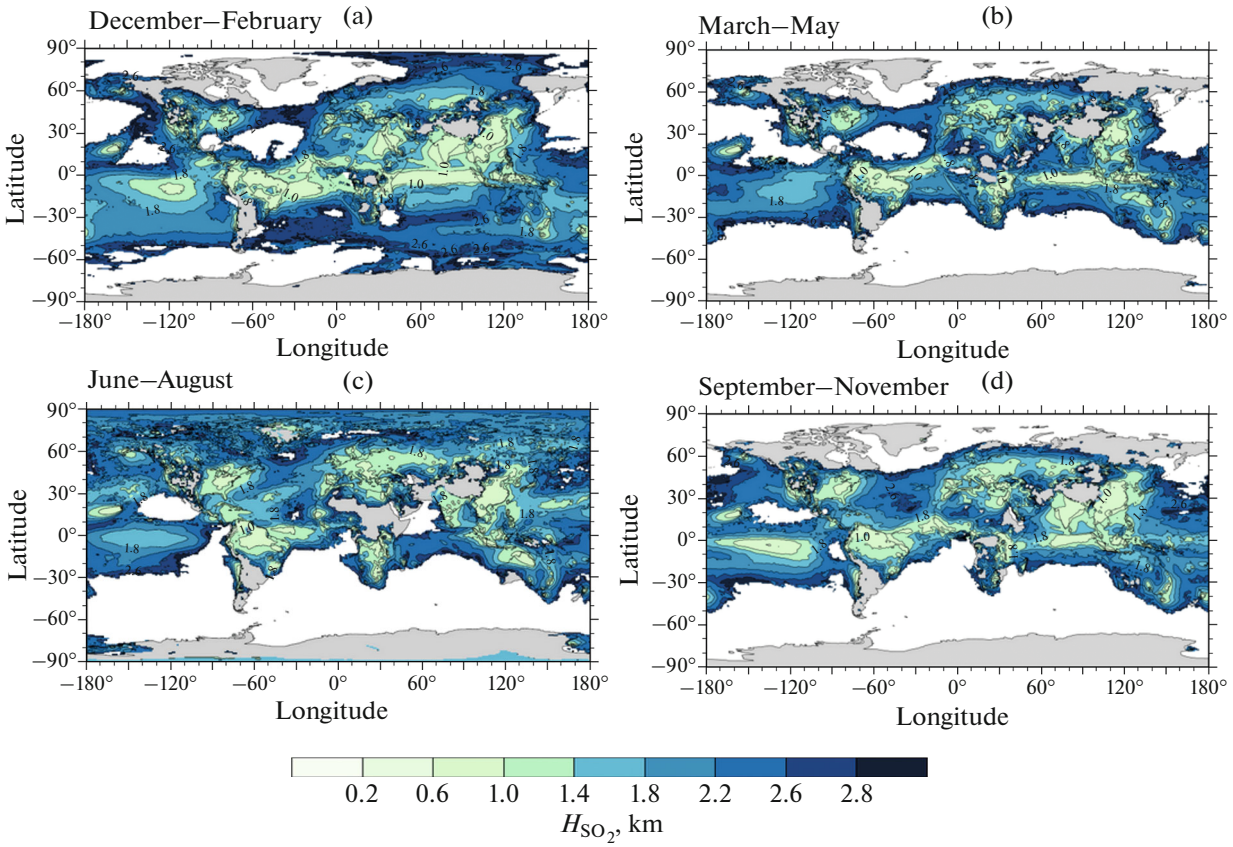

Fig. 3. Same as in Fig. 1 for the vertical scale of sulfur dioxide concentration (a) in Nortern Hemisphere winter, (b) in spring, (c) in summer, and (d) in autumn.

99% are 0.400, 0.468, and 0.590, respectively. As a consequence, isolines in Fig. 5 (and, further, in Fig. 8) approximately correspond to boundaries of regions with the corresponding statistical significance level. In addition, we note that it is not required to use methods by which the statistical significance of coefficients of time correlations between fields is analyzed, e.g., the Walker test or control of the false discovery rate [26]; in fact, we merely seek spatially coherent regions with statistically significant relations between individual time series (not between fields).

Table 1. Coefficients of spatial correlation between different H_Y

Scale height	H_{PBL}	H_{vap}	H_{SO_2}	H_{SO_4}
H_{PBL}	1	−0.59	0.44	0.18
H_{vap}		1	−0.16	−0.02
H_{SO_2}			1	0.44
H_{SO_4}				1

When calculating the spatial correlations, values of variables in the grid cells were averaged with weights corresponding to the area of the horizontal data cell.

The areas of significant negative correlations between H_{PBL} and H_{vap} are situated in regions with the highest water content in the lower troposphere (Fig. 7). Moreover, the seasonal variation of boundaries of these areas is similar to the seasonal variation of specific humidity.

With reference to the abovementioned, it should be noted that the high water content of the PBL favors the development of moist convective processes. Moist convection favors the formation of intense precipitations, which, in turn, increases buoyancy of air convective elements and additionally intensifies the developing convection [27]. Therefore, the negative correlation between H_{PBL} and H_{vap} in moist regions of the tropics can be associated with convective activity. At the same time, the negative correlation between H_{PBL} and H_{vap} in these regions can point to the inapplicability of the Einstein–Stokes theory for effective diffusion in the PBL in view of the influence of mesoscale vortices. In addition, the abovementioned correlation is almost absent over land (see Fig. 5). The small areas where it turns out to be significant are characterized by a strong influence of maritime air masses as, for example, in the east of Europe in winter (which is related to the moisture transfer from the ocean by storm tracks) or over the Hindustan Peninsula in summer (appar-

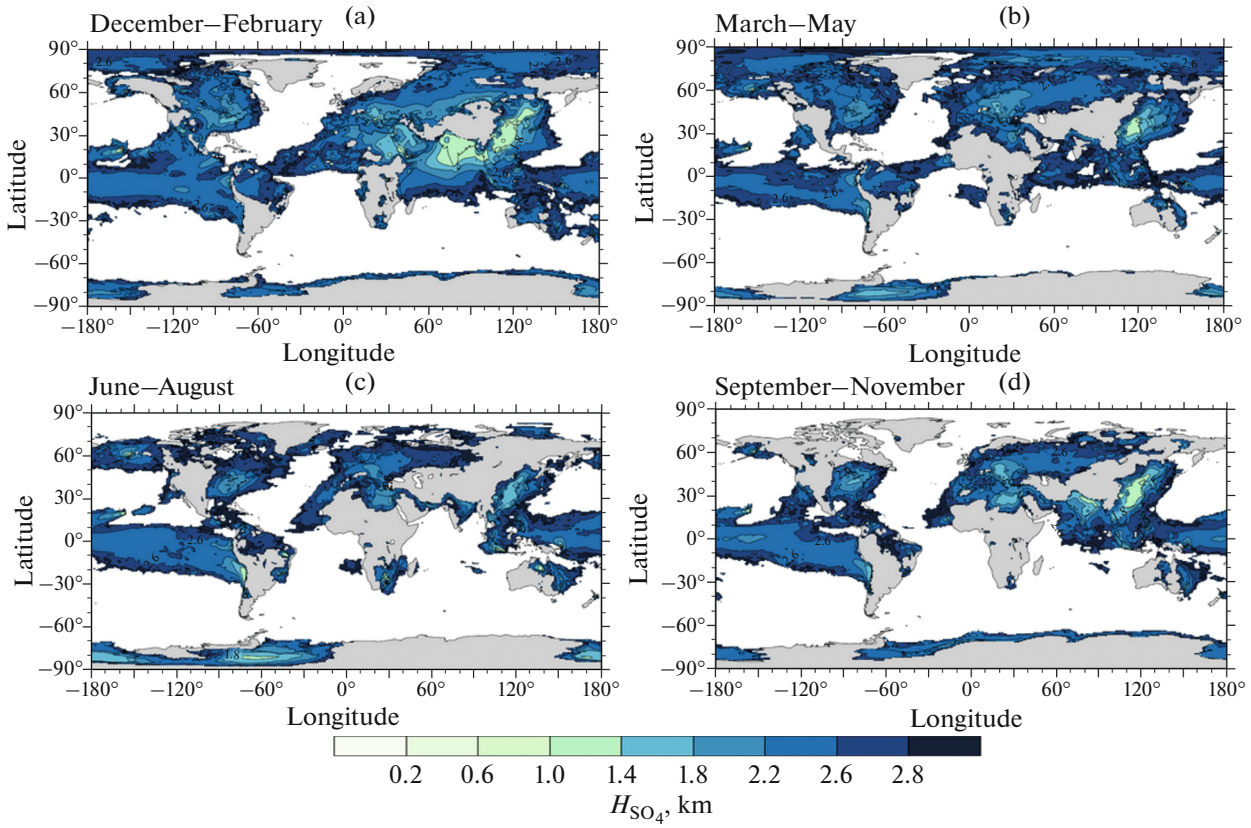

Fig. 4. Same as in Fig. 1 for the scale height of sulfates.

ently, due to the influence of the monsoonal circulation). It should be noted that at least the second area is small and can be associated with the false discovery of statistical methods [26].

2.3. Correlation between Scale Heights of Sulfur Dioxide and Sulfate Aerosols

In some regions, a statistically significant correlation between scale heights of sulfur dioxide and sulfate aerosols is revealed (Fig. 8). It is statistically significant but only in regions with strong aerosol contamination in the south and southeast of Eurasia and is less significant in Europe. Over continents in the Northern Hemisphere, this is more pronounced in the warm period of the year than in the cold period.

The relatively low level of statistical significance of the correlation between H_{SO_2} and H_{SO_4} can be related, in particular, to disadvantages in calculation of these scale heights in terms of regression dependences (see Section 1). For example, reanalysis data can be of relatively low quality over mountain regions. Over regions with a relatively low content of sulfur compounds in the troposphere, calculation of coefficients of the corresponding linear regression can be impeded because of the low level of statistical data provision. In other words, the range of values of such data is not large enough and, as a consequence, the effects of noisiness related both to inaccuracy of the data and to processes deviating the profiles $q_{SO_2}(z)$ and $q_{SO_4}(z)$ from the chosen exponential dependence begin to play a part.

Nevertheless, the positive correlation between H_{SO_2} and H_{SO_4} manifests itself in most regions with severe atmospheric contamination by sulfur compounds. In particular, the slope α of the interannual linear regression in which H_{SO_2} is the predictor and H_{SO_4} is the predictand is positive in all such regions (Fig. 9). Moreover, its values are sufficiently spatially homogeneous and vary within the range of ~1–3. As a consequence, the dependence derived is statistically stable.

CONCLUSIONS

In this work, a global analysis of geographical features of vertical profiles of specific humidity and concentrations of sulfur dioxide and sulfate aerosols has been carried out based on CAMS reanalysis data for 2003–2020. The profile of the PBL height has been also analyzed based on ERA5 reanalysis data for the

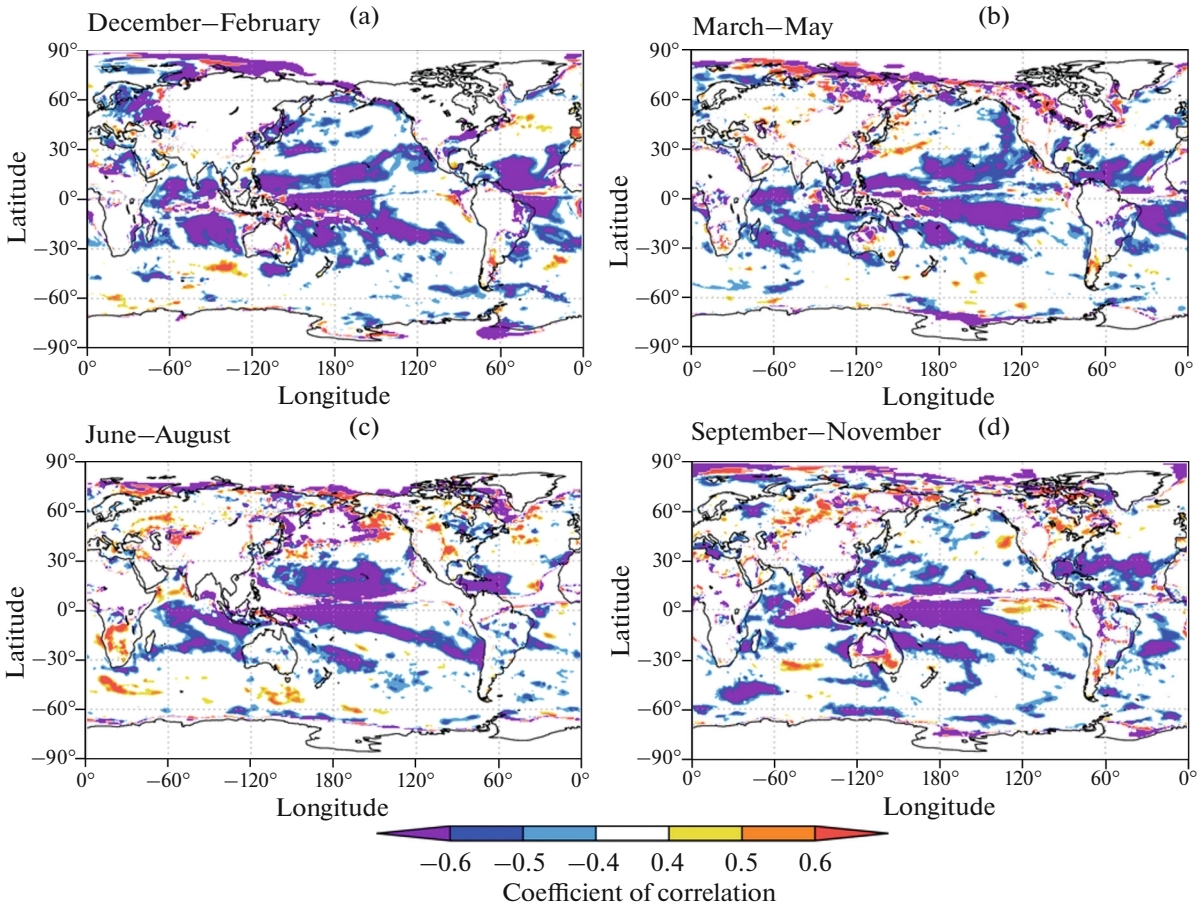

Fig. 5. Maps of coefficients of correlations between seasonal average values of H_{vap} and H_{BL} for (a) Nortern Hemisphere winter, (b) spring, (c) summer, and (d) autumn.

same time interval. The scale height H_Y which corresponds to a decrease in substance concentration by a factor of e was used as the main analyzed characteristic of the abovementioned profiles.

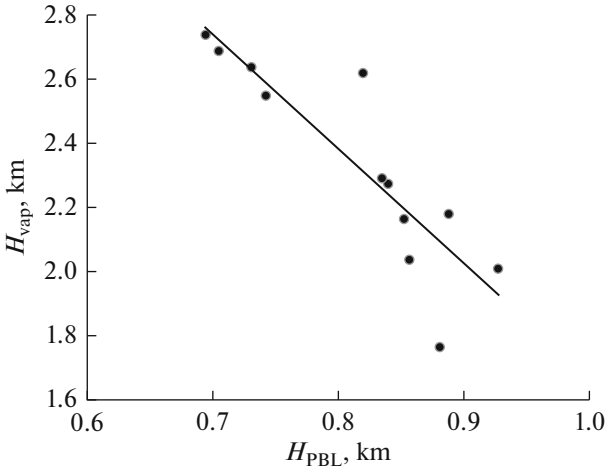

Fig. 6. Correlations between seasonal average (December–February) values of H_{vap} and H_{BL} for the point with the coordinates 0° N and 180° E.

Height maxima of the upper PBL boundary are observed in regions of the predominating cyclonic gyre, in storm tracks, and in regions of monsoonal circulation in summer. For the vertical scale of the specific humidity profile, minima have been revealed in regions of subtropical gyres with predominant large-scale subsidence of air masses. The scale height of SO_2 is characterized by spatial minima apparently related to oxidation of this substance. For H_{SO_4}, a spatial minimum has been revealed over the ocean near southeast Asia.

A statistically significant negative correlation between the PBL thickness and the vertical scale for specific humidity has been revealed in moist regions of the tropics. This correlation can point to the inapplicability of the Einstein–Stokes theory to effective diffusion in the PBL due to the influence of mesoscale vortices on it.

It should be noted that, in spite of the commonly accepted assumptions used when deriving formulas (3) and (4), the negative correlation between H_{PBL} and H_{vap} seems to be contradicting intuitive understanding: a higher PBL is usually associated with intense convection in it, which, supposedly, should also favor the propagation of atmospheric impurities to greater

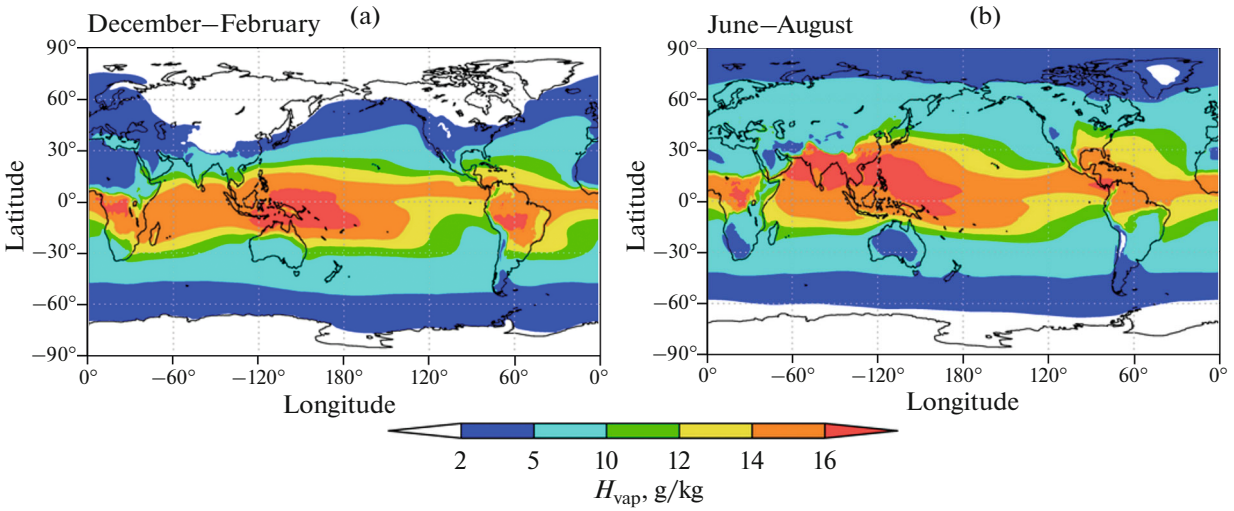

Fig. 7. Seasonal average values of specific humidity (a) in Northern Hemisphere winter and (b) in summer at an isobaric level of 950 hPa according to ERA5 reanalysis data.

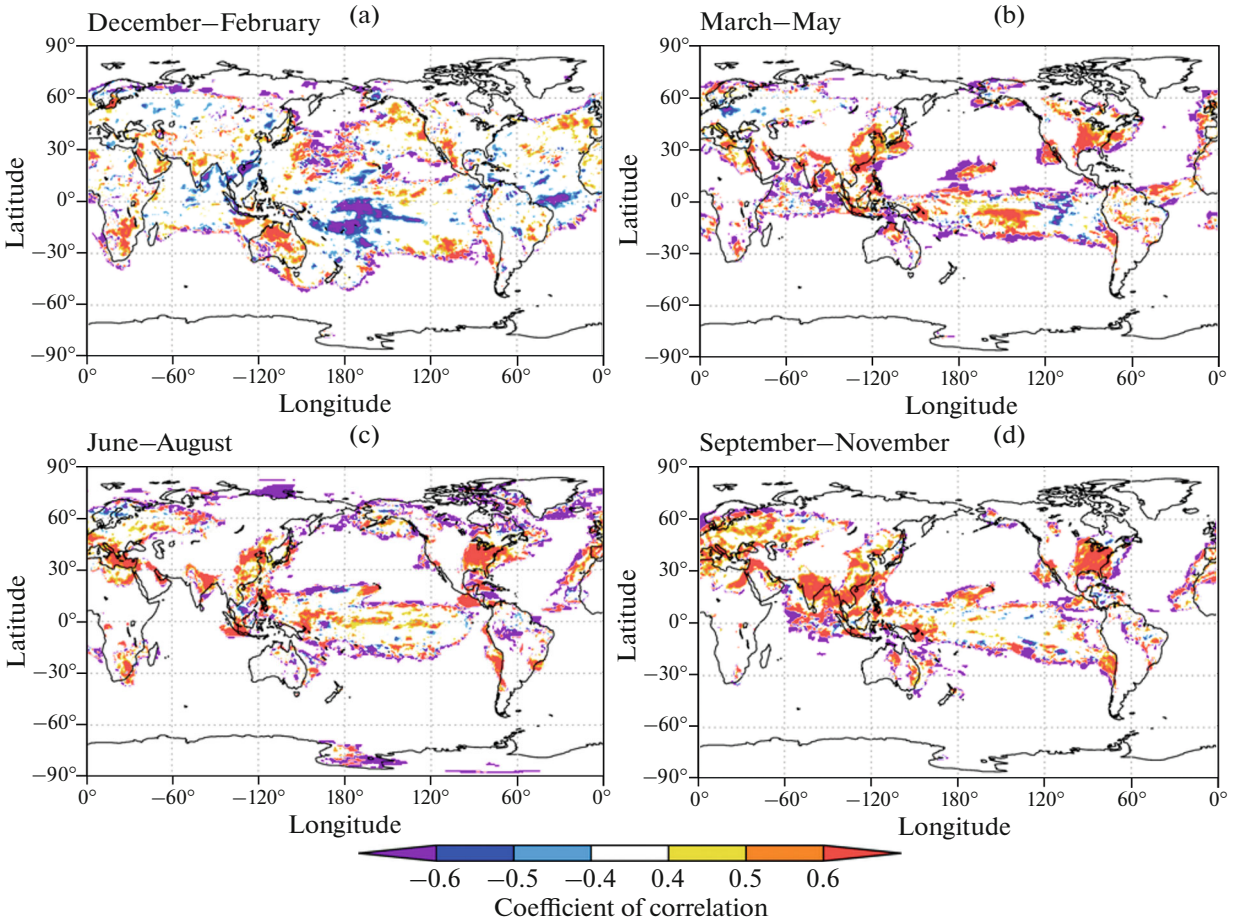

Fig. 8. Coefficients of correlation between H_{SO_2} and H_{SO_4} for (a) Northern Hemisphere winter, (b) spring, (c) summer, and (d) autumn.

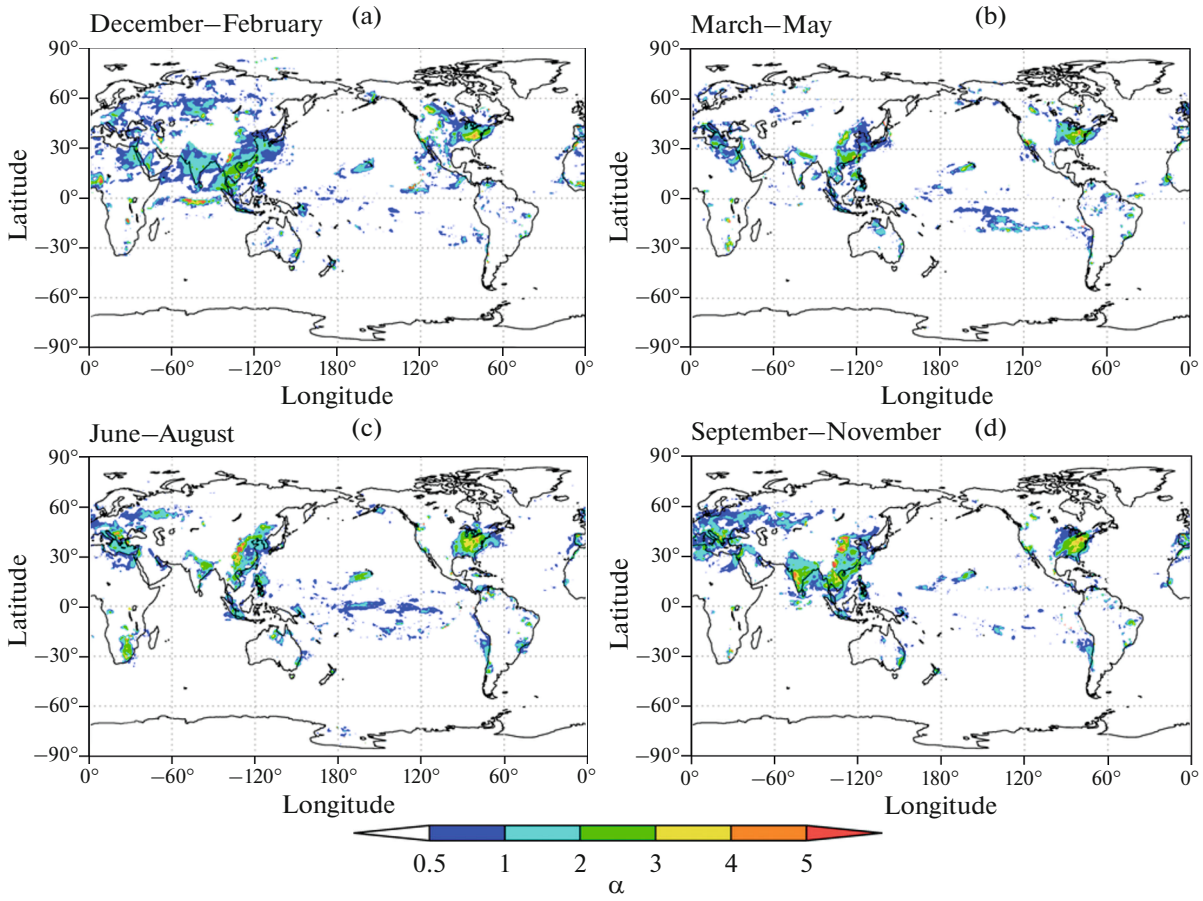

Fig. 9. Same as in Fig. 8 but for the coefficient α of interannual linear regression of H_{SO_4} on H_{SO_2} for (a) Northern Hemisphere winter, (b) spring, (c) summer, and (d) autumn.

heights. However, such intense convection is usually accompanied by intense precipitation. As seen from (3) and (4), the influence of diffusion on H_{PBL} and H_{vap} is opposite in sign. Physically, this is related to the fact that the direction of the diffusion flow is determined by the gradient of the mean concentration of the transferred variable. Since the wind speed in the PBL increases with height and concentration of impurities emitted from the Earth's surface decreases, the diffusion flows of momentum and these impurities are oppositely directed.

A positive correlation between scale heights of sulfur dioxide and sulfates has also been revealed. The correlation manifests itself most significantly in regions of strong contamination of the lower troposphere by these substances. In southern and southeastern Eurasia, this correlation can be related (at least partially) to the seasonal maximum of H_{BL}. However, it also manifests itself in other regions with contamination of the lower troposphere by sulfur compounds—in Europe and in the east of North America. As a consequence, its appearance is affected by processes not related directly to the seasonal maximum of the PBL thickness.

It should be noted that under other assumptions about, e.g., the vertical structure of parameters of the problem, one can also derive alternative relationships for vertical profiles of impurities in the lower troposphere. In particular, as shown in [28], if the diffusion coefficient in the PBL linearly depends on height,

$$K_{z,Y} = l_{z,Y,0}(z + z_0), \tag{5}$$

where the coefficient $\lambda_{z,0}$ is equal to the product of friction velocity and von Kármán's constant and z_0 is the roughness height, then the vertical concentration profile of impurity Y has the form

$$q_Y(z) = q_Y(0)\left(z/z_0 + 1\right)^{-S_Y}, \tag{6}$$

where $S_Y = u_{T,Y}/\lambda_{z,Y,0}$. The quantity $H_Y = HS_Y$ can also be treated as a characteristic of the vertical profile of an impurity in the lower troposphere. However, when passing from the relationship for the ground level concentration of a substance to the relationship for its total content in the tropospheric column, integration should be performed up to a certain height dH_Y, where d is a number (depending on S_Y) in the range from 1 to 10 with an additional condition $0 < S_Y < 1$. Under a more severe condition $S_Y \ll 1$,

$$B_Y = q_Y(0)z_0 dH_Y. \quad (7)$$

As a consequence, first, H_Y turns out to be ambiguously determined (in view of the dependence on d); second, information about the type of the underlying surface (value of the parameter z_0) is required. For this reason, such an approach is not used in this work.

The results are useful both for a concise representation of geographic features of the vertical distribution of impurities in the lower troposphere and from the viewpoint of numerical simulation of climate-forming processes in the atmosphere in the case of specifying such vertical distributions in the form of universal (exponential) dependences on the vertical coordinate in simplified models of the Earth system. In particular, the relationship between H_{SO_2} and H_{SO_4} can be used in the further development of the ChAP scheme [4].

ACKNOWLEDGMENTS

We are deeply grateful to I.I. Mokhov and O.G. Chkhetiani for useful discussion and to the anonymous reviewer for remarks to the previous version of the paper.

FUNDING

Statistical analysis of parameters describing the relation between the vertical distribution of atmospheric impurities and the thickness of the planetary boundary layer, as well as between the parameters themselves, was supported by the Russian Science Foundation (project no. 20-62-46056). Analysis of the spatial distribution of the planetary boundary layer thickness and parameters of the vertical distribution of atmospheric impurities was supported by the Russian Science Foundation (project no. 19-17-00240).

CONFLICT OF INTEREST

The authors declare that they have no conflicts of interest.

REFERENCES

1. R. Jaenicke, "Tropospheric aerosols," in *Aerosol-Cloud-Climate Interactions* (Academic Press, San Diego, 1993), vol. 54, p. 1–31.
2. P. Warneck, *Chemistry of the Natural Atmosphere* (Academic Press, San Diego, 2000).
3. A. Wypych and B. Bochenek, "Vertical structure of moisture content over Europe," Adv. Meteorol. **2018**, 3940503 (2018). https://doi.org/10.1155/2018/3940503
4. A. V. Eliseev, R. D. Gizatullin, and A. V. Timazhev, "ChAP 1.0: A stationary tropospheric sulfur cycle for Earth system models of intermediate complexity," Geosci. Mod. Devel. **14** (12), 7725–7747 (2021). https://doi.org/10.5194/ gmd-14-7725-2021
5. V. K. Petoukhov, I. I. Mokhov, A. V. Eliseev, and V. A. Semenov, *The IAP RAS Global Climate Model* (Dialogue-MSU, Moscow, 1998).
6. V. Petoukhov, A. Ganopolski, V. Brovkin, M. Claussen, A. Eliseev, K. Kubatzki, and S. Rahmstorf, "CLIMBER-2: A climate system model of intermediate complexity. Part I: Model description and performance for present climate," Clim. Dyn. **16** (1), 1–17 (2000).
7. M. Claussen, L. A. Mysak, A. J. Weaver, M. Crucifix, T. Fichefet, M.-F. Loutre, S. L. Weber, J. Alcamo, V. A. Alexeev, A. Berger, R. Calov, A. Ganopolski, H. Goosse, G. Lohmann, F. Lunkeit, I. I. Mokhov, V. Petoukhov, P. Stone, and Z. Wang, "Earth system models of intermediate complexity: Closing the gap in the spectrum of climate system models," Clim. Dyn. **18** (4), 579–586 (2002). https://doi.org/10.1007/s00382-001-0200-1
8. I. I. Mokhov, A. V. Eliseev, P. F. Demchenko, V. Ch. Khon, M. G. Akperov, M. M. Arzhanov, A. A. Karpenko, V. A. Tikhonov, A. V. Chernokulsky, and E. V. Sigaeva, "Climate changes and their assessment based on the IAP RAS global model simulations," Dokl. Earth Sci. **402** (4), 591–595 (2005).
9. I. I. Mokhov, A. V. Eliseev, and V. V. Guryanov, "Model estimates of global and regional climate changes in the holocene," Dokl. Earth Sci. **490** (1), 23–27 (2020).
10. I. I. Mokhov and A. V. Eliseev, "Modeling of global climate variations in the 20th-23rd centuries with new RCP scenarios of anthropogenic forcing," Dokl. Earth Sci. **443** (2), 532–536 (2012)
11. T. L. Frolicher, C. D. Jones, J. Rogelj, H. D. Matthews, K. Zickfeld, V. K. Arora, N. J. Barrett, V. Brovkin, F. A. Burger, M. Eby, A. V. Eliseev, T. Hajima, P. B. Holden, A. Jeltsch-Thommes, C. Koven, N. Mengis, L. Menviel, M. Michou, I. I. Mokhov, A. Oka, J. Schwinger, R. Seferian, G. Shaffer, A. Sokolov, K. Tachiiri, J. Tjiputra, A. Wiltshire, and T. Ziehn, "Is there warming in the pipeline? A multi-model analysis of the zero emissions commitment from CO_2," Biogeosciences **17** (11), 2987–3016 (2020). https://doi.org/10.5194/bg-17-2987-2020
12. J. R. Holton, *An Introduction To Dynamic Meteorology* (Academic Press, San Diego, 2004).
13. J. O. Hirschfelder, C. F. Curtiss, and R. B. Bird, *The Molecular Theory of Gases and Liquids* (John Wiley, New York; Chapman & Hall, London, 1954).
14. A. V. Eliseev, M. Zhang, A. I. Skorokhod, R. D. Gizatullin, A. V. Altukhova, and Yu. P. Perevedentsev, "Impact of sulfur dioxide on the terrestrial carbon cycle," Izv., Atmos. Ocean. Phys. **55** (1), 38–49 (2019).
15. V. E. Zuev and G. A. Titov, *Atmospheric Optics and Climate* (Spektr, Tomsk, 1996) [in Russian].
16. E. M. Feigel'son, *Radiation Exchange and Clouds* (Gidrometeoizdat, Leningrad, 1970) [in Russian].
17. R. Charlson, S. Schwartz, J. Hales, R. Cess, J. Coackley, J. Hansen, and D. Hofmann, "Climate forcing by anthropogenic aerosols," Science **255**, 423–430 (1992). https://doi.org/10.1126/science.255.5043.423
18. V. Naik, S. Szopa, B. Adhikary, P. Artaxo, T. Berntsen, W. D. Collins, S. Fuzzi, L. Gallardo, A. Kiendler Scharr, Z. Klimont, H. Liao, N. Unger, and P. Zanis, "Short-lived climate forcers," in *Climate Change 2021:*

The Physical Science Basis (Cambridge University Press, Cambridge, 2021).

19. S. M. Semenov, I. M. Kunina, and B. A. Kukhta, "Comparison between anthropogenic changes in O_3, SO_2, and CO_2 in Europe based on ecological criterion," Dokl. Akad. Nauk **361** (2), 275–279 (1998).
20. A. V. Eliseev, "Impact of tropospheric sulphate aerosols on the terrestrial carbon cycle," Glob. Planet. Change **124**, 30–40 (2015).
21. A. V. Eliseev, "Influence of sulfur compounds on the terrestrial carbon cycle," Izv., Atmos. Ocean. Phys. **51** (6), 599–608 (2015).
22. A. Inness, M. Ades, A. Agusti-Panareda, J. Barre, A. Benedictow, A.-M. Blechschmidt, J. Dominguez, R. Engelen, H. Eskes, J. Flemming, V. Huijnen, L. Jones, Z. Kipling, S. Massart, M. Parrington, V.pH. Peuch, M. Razinger, S. Remy, M. Schulz, and M. Suttie, "The CAMS reanalysis of atmospheric composition," Atmos. Chem. Phys. **19** (6), 3515–3556 (2019). https://doi.org/10.5194/ acp-19-3515-2019
23. H. Hersbach, B. Bell, P. Berrisford, S. Hirahara, A. Horanyi, J. Munoz-Sabater, J. Nicolas, C. Peubey, R. Radu, D. Schepers, A. Simmons, C. Soci, S. Abdalla, X. Abellan, G. Balsamo, P. Bechtold, G. Biavati, J. Bidlot, M. Bonavita, G. De Chiara, P. Dahlgren, D. Dee, M. Diamantakis, R. Dragani, J. Flemming, R. Forbes, M. Fuentes, A. Geer, L. Haimberger, S. Healy, R. J. Hogan, E. Holm, M. Janiskova, S. Keeley, P. Laloyaux, P. Lopez, C. Lupu, G. Radnoti, P. de Rosnay, I. Rozum, F. Vamborg, S. Villaume, and J.-N. Thepaut, "The ERA5 global reanalysis," Quant. J. Roy. Meteorol. Soc. **146** (730), 1999–2049 (2020). https://doi.org/10.1002/qj.3803
24. D. H. P. Vogelezang and A. A. M. Holtslag, "Evaluation and model impacts of alternative boundary-layer height formulations," Bound.-Lay. Meteorol. **81** (3), 245–269 (1996). https://doi.org/10.1007/BF02430331
25. D. Coumou, V. Petoukhov, and A. V. Eliseev, "Three-dimensional parameterizations of the synoptic scale kinetic energy and momentum flux in the Earth's atmosphere," Nonlin. Proc. Geophys. **18** (6), 807–827 (2011).
26. D. S. Wilks, ""Field Significance" and the "False Discovery Rate"," J. Appl. Meteorol. Climatol. **45** (9), 1181–1189 (2006). https://doi.org/10.1175/JAM2404.1
27. W. W. Grabowski and H. Morrison, "Supersaturation, buoyancy, and deep convection dynamics," Atmos. Chem. Phys. **21** (18), 13997–14018 (2021). doi 10. 5194/acp-21-13997-2021
28. P. A. Taylor, "Constant flux layers with gravitational settling: Links to aerosols, fog and deposition velocities," Atmos. Chem. Phys. **21** (24), 18263–18269 (2021). https://doi.org/10.5194/acp-21-18263-2021

Translated by A. Nikol'skii